Electric-field controlled spin in bilayer triangular graphene quantum dots

A. D. Güçlü,[1,*] P. Potasz,[1,2,*] and P. Hawrylak[1]
[1]*Institute for Microstructural Sciences, National Research Council of Canada, Ottawa, Canada*
[2]*Institute of Physics, Wroclaw University of Technology, Wroclaw, Poland*
(Received 21 June 2011; published 25 July 2011)

We present theoretical results based on mean-field and exact many-body approaches showing that in bilayer triangular graphene quantum dots with zigzag edges, the magnetism can be controlled by an external vertical electric field. We demonstrate that without electric field, the spins of the two layers of the quantum dot interact ferromagnetically. At a critical value of the electric field, the total spin of the bilayer structure can be turned off or reduced to a single-localized spin, a qubit isolated from contacts and free from interaction with nuclear spins.

DOI: 10.1103/PhysRevB.84.035425 PACS number(s): 73.63.Kv, 73.22.Pr

I. INTRODUCTION

Graphene exhibits unusual electronic properties[1–8] including relativistic nature of quasiparticles, sublattice pseudospin, and zero-energy band gap. The application of graphene for logic devices requires opening of the band gap which can be achieved by either size quantization,[9–20] chemical modification,[21] addition of a second layer and application of an external electric field,[22–30] or size quantization in bilayer graphene nanostructures.[31–34] In particular, when graphene is reduced to a triangular quantum dot with zigzag edges,[10] sublattice symmetry is broken, size-dependent energy gap is open, and a band of degenerate states at the Fermi level is created leading to finite macroscopic spin polarization.[13–20] This allows simultaneous size, shape, and edge engineering of magnetic, electrical, and optical properties in a single material graphene.[16]

In this work, we develop a theory of electronic and magnetic properties of bilayer triangular graphene quantum dots with zigzag edges. We show that the magnetic moment of bilayer triangular graphene quantum dots can be controlled by the vertical electric field. Without the electric field, the magnetic moments of the two layers are shown to be coupled ferromagnetically. Using configuration interaction and mean-field calculations based on tight-binding model, we demonstrate that the ferromagnetism can be either turned off or reduced to a single electron/hole spin. The single electron spin is hence isolated in a charge neutral structure by the application of an electric field, independent of the size of the quantum dot and without decoherence due to contacts. The electric-field control of the ferromagnetism[35] and isolation of a single spin opens new applications in spintronics and quantum information processing.[36–40]

Our paper is organized as follow. In Sec. II, we describe the tight-binding model of the bilayer system and discuss the effect of electric field in the single particle picture. In Sec. III, we present mean-field Hubbard results. In Sec. IV, we use a Hartree-Fock-configuration-interaction approach to study correlation and long-range interaction effects for charge neutral and charged systems. Finally, we summarize our results in Sec. V.

II. TIGHT-BINDING MODEL

Figure 1(a) shows two possibilities for building a bilayer triangular graphene quantum dot (BTGQD) using two single-layer triangular quantum dots (TGQDs) of comparable sizes, with zigzag edges. The stability of TGQDs to defects was established in Refs. 17 and 18. We consider AB Bernal stacking, where the A sublattice of the top layer (A2, shown in blue color online) is on top of the B sublattice of the bottom layer (B1, shown in red color online). On the left hand side, the two TGQDs are of the same size. In this configuration, however, not all the A2 atoms have a B1 partner as required by Bernal stacking. A more natural configuration choice is shown on the right hand side of Fig. 1(a). The top layer triangle has its floating atoms removed, making it smaller than the bottom layer triangle. Such a bilayer construction has the interesting property of having an odd number of degenerate states at the Fermi level independent of its size, allowing to isolate a single spin in a charge neutral structure. This is illustrated in Fig. 1(b), where the spin density isosurfaces are shown for zero electric field (left hand side) and finite electric field (right hand side), as obtained from our tight-binding-based configuration interaction calculations explained in detail in Sec. IV. When the electric field is off, both layers have a finite magnetic moment, as in single layer triangles,[14–20] differing by one spin due to the size difference of the two triangles. The magnetic moments of the two layers are coupled ferromagnetically, in agreement with Lieb's theorem[41] which applies for Bernal stacking. When a sufficiently high electric field is applied, electrons from the lower layer reduce their energy by transferring to the top layer filling up all the available spin up and down zero-energy states, leaving behind one single spin. We note that, the depolarization effect described above is robust against defects, since Lieb's theorem[41] guarantees magnetization of individual layers and ferromagnetic coupling between them, as long as the biparticity of the honeycomb lattice is not distorted. To understand the effect of strong distortion of the biparticity or the honeycomb structure of the lattice, future work is necessary. Another type of defect can be due to charging from the environment which we will discuss in Sec. IV.

We have confirmed the above depolarization picture through calculations with varying levels of accuracy. As a first step, we diagonalize the tight-binding Hamiltonian given by

$$H_{TB} = \sum_{ij\sigma} \tau_{ij} c^{\dagger}_{i\sigma} c_{j\sigma} + \sum_{i\sigma} V_i c^{\dagger}_{i\sigma} c_{i\sigma}, \qquad (1)$$

where the operator $c^{\dagger}_{i\sigma}$ creates an electron on a p_z orbital on

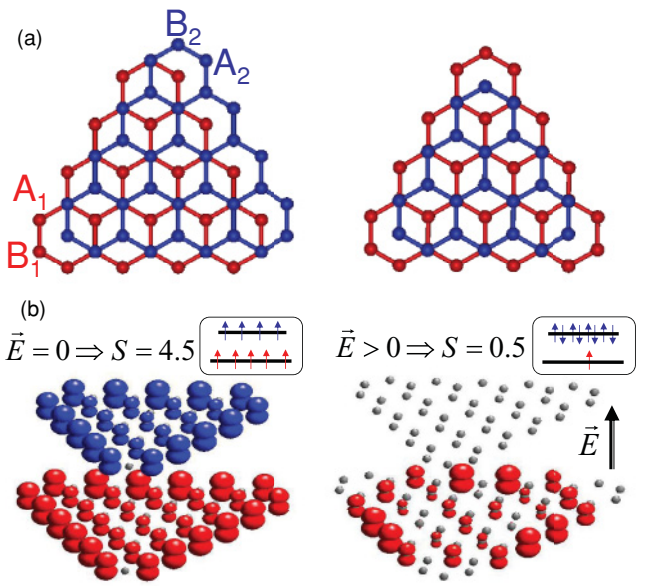

FIG. 1. (Color online) Bilayer triangular graphene quantum dot with zigzag edges. (a) Structure constructed using two single-layer quantum dots with equal sizes (on the left) and different sizes (on the right). (b) Isosurface plot of the spin density $\rho_\uparrow - \rho_\downarrow$ for with and without electric field **E**, obtained from configuration interaction calculations.

site i with spin σ. The tight-binding parameters τ_{ij} are fixed to their bulk values $t = -2.8$ eV for in-plane nearest neighbors i and j and $t_\perp = 0.4$ eV for interlayer hopping between A2 and B1 atoms. The effect of the potential difference induced by an external perpendicular electric field **E** is taken into account through $V_i = -\Delta V/2$ for the bottom layer atoms and $V_i = \Delta V/2$ for the top layer atoms. Figure 2(a) shows the energy spectrum near the Fermi level for $\Delta V = 0$ for a BTGQD consisting of 622 atoms in the bottom and 573 atoms in the top layer. If we take $t_\perp = 0$, the two triangles are decoupled and we find 22 zero-energy states in the bottom layer and 21 zero-energy states in the top layer, for a total of 43 zero-energy states, consistent with previous work on single-layer TGQDs.[14–20] Turning on $t_\perp$ to 0.4 eV does not affect the zero-energy states. The effect of applying an electric field, e.g., $\Delta V = 0.4$ eV, is shown in Fig. 2(b). The energy of the 21 zero-energy states corresponding to the top layer is pushed up by 0.4 eV with respect to the bottom layer zero-energy states. Note that the bottom layer zero-energy states do not experience any dispersion unlike the top layer zero-energy states. This is due to the fact that they lie strictly on A1 sites which are not coupled to the top layer, whereas the top layer zero-energy states, which lie on B2, do couple to the bottom layer. The ability of controlling the relative position of zero-energy states gives an interesting opportunity to control the charge and spin of the zero-energy states, expected to be spin polarized for $\Delta V = 0$ according to Lieb's theorem.[41]

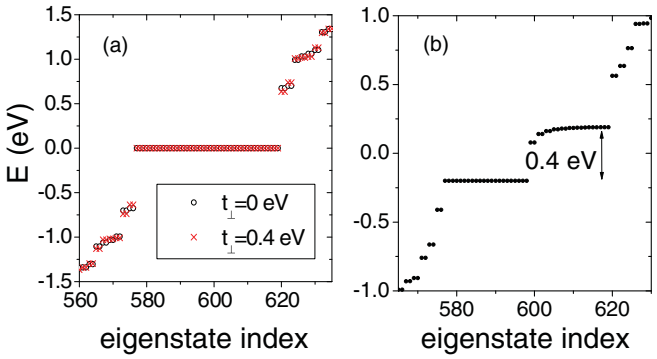

FIG. 2. (Color online) Single-particle tight-binding spectrum. (a) The bilayer quantum dot consisting of 1195 atoms has 43 zero-energy states. (b) When an electric field is applied, the degeneracy between the 21 top layer zero-energy states and 22 bottom layer zero-energy states is lifted.

III. MEAN-FIELD HUBBARD RESULTS

The magnetic properties of BTGQD structures as a function of applied electric field can be studied by solving the Hubbard model within the self-consistent mean-field approach:

$$H_{MF} = \sum_{ij\sigma} \tau_{ij} c^\dagger_{i\sigma} c_{j\sigma} + \sum_{i\sigma} V_i n_{i\sigma} + U \sum_{i\sigma} \left(\langle n_{i\sigma} \rangle - \frac{1}{2} \right) n_{i\sigma}, \tag{2}$$

where U is the on-site Hubbard term taken to be 2.75 eV, screened by a factor of ~6 from the bare Coulomb potential calculated numerically using Slater orbitals.[15] The mean-field Hubbard approach with similar values of U was previously applied to TGQDs (Ref. 19) giving a good agreement with density-functional calculations. First, we study a small BTGQD of 107 atoms and 9 zero-energy states. Figure 3(a) shows the energies for different total spin projection S^z with respect to the energy of the ferromagnetic configuration, $S^z = 9/2$. At $\Delta V = 0$, the degenerate band of zero-energy states is polarized: all nine electrons occupying the nine zero-energy states have their spins aligned ferromagnetically as explicitly shown in Fig. 3(b). Although the first excited state obtained from the Hubbard model is antiferromagnetic with

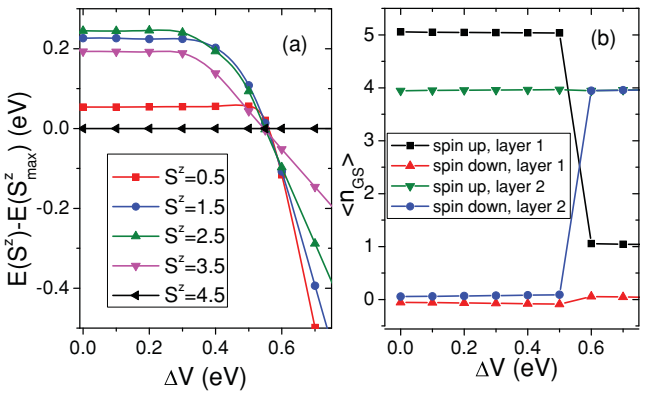

FIG. 3. (Color online) Mean-field Hubbard results for a system of 107 atoms and 9 zero-energy states. (a) Energies of lowest energy states with different total spin projection S^z as a function of potential difference ΔV_c between the layers, with respect to the ferromagnetic configuration $S^z_{\max} = 4.5$. (b) Ground state spin population for a given layer and spin.

the polarization of the bottom layer opposite to the polarization of the top layer, a full treatment of the correlation effects shows that (see below) low lying excited states have more complex spin structures. The Hubbard model is, however, useful for estimating the critical value V_c where phase transition occurs. As ΔV is increased, the electrons lying on the bottom layer zero-energy states are forced to flip their spin and tunnel to the top layer zero-energy states. At around $\Delta V_c = 0.55$ eV, such charge transfers occur abruptly, leading to a decrease of the magnetization of the system. As a result, all top layer zero-energy states become doubly occupied, leaving exactly one single spin in the bottom layer zero-energy states. We note that one can also isolate a single hole spin in the bottom layer by applying a reverse electric field, thus pushing the electrons from the top layer to the bottom layer, occupying all states except one. It is thus possible to isolate a single electron or hole spin in a neutral BTGQD by applying an external electric field.

The procedure of isolating single electron or hole should occur regardless of the size of the system since the top layer has always one less zero-energy state than the bottom one. In order to investigate the size dependence, in Fig. 4(a) we show the energy difference between the ferromagnetic and antiferromagnetic (FM-AFM) states calculated in the mean-field Hubbard approximation as a function of applied voltage for several sizes up to 1507 atoms. We note that, due to the unusually high degeneracy of the states, self-consistent iterations occasionally get trapped in local energy minima. We have thus repeated the calculations several times using different initial conditions and/or convergence schemes to assure that the correct ground state was reached. As expected, at $\Delta V = 0$, the FM-AFM gap increases with the size of the system N. In fact, the FM-AFM gap energy per N_{side}, the number of side atoms on the top layer (N_{side}) (equal to the number of interlayer bonds on the edges), approaches a constant value of 14.3 meV as shown in Fig. 4(b). However, the FM-AF transition voltage V_c decreases with the system size as can be seen from Fig. 4(c). For the largest system size studied, $N = 1507$, we obtain $\Delta V_c = 0.345$ eV, which corresponds to an electrical field of $\sim$1 V/nm, a value within experimental range.[26]

IV. CONFIGURATION INTERACTION RESULTS AND EFFECT OF CHARGING

We now test the predictions of the mean-field Hubbard model by including long-range interaction and correlation effects, which is computationally feasible for the system size studied in Fig. 3. We first solve a Hartree-Fock generalization of the Eq. (2), but with empty zero-energy states:[15]

$$H_{HF} = \sum_{ij\sigma} \tau_{ij} c^\dagger_{i\sigma} c_{j\sigma} + \sum_{i\sigma} V_i n_{i\sigma} + \sum_{il\sigma} \sum_{jk\sigma'} \left(\rho_{jk\sigma'} - \rho^{\text{bulk}}_{jk\sigma'}\right) \times \left(\langle ij|V_{ee}|kl\rangle - \langle ij|V_{ee}|lk\rangle \delta_{\sigma,\sigma'}\right) c^\dagger_{i\sigma} c_{l\sigma}, \quad (3)$$

where the tight-binding term now includes the intralayer next-nearest neighbor hopping $t = -0.1$ eV, interlayer next-nearest hoppings $\gamma_3 = 0.3$ eV and $\gamma_4 = 0.15$ eV.[29] The terms ρ and ρ^{bulk} are quantum dot and bulk density matrices, respectively.[15] The two-body Coulomb matrix elements $\langle ij|V_{ee}|kl\rangle$ computed using Slater p_z orbitals include on-site interactions, all scattering and exchange terms within next-nearest neighbors, and all long-range direct interactions. We have previously tested the validity of our approach by comparing to density functional calculations and obtained good agreement.[15] After diagonalizing the Hartree-Fock Hamiltonian, we obtain Hartree-Fock quasiparticles denoted by the creation operator $b^\dagger_{p\sigma}$, with eigenvalues ϵ_p and eigenfunctions $|p\rangle$. We can now fill the new quasiparticle zero-energy states with electrons and solve the many-body Hamiltonian given by

$$H = \sum_{p\sigma} \epsilon_p b^\dagger_{p\sigma} b_{p\sigma} + \frac{1}{2} \sum_{pqrs\sigma\sigma'} \langle pq|V_{ee}|rs\rangle b^\dagger_{p\sigma} b^\dagger_{q\sigma'} b_{r\sigma'} b_{s\sigma}. \quad (4)$$

Figure 5(a) shows the evolution of spin states for the same system studied in Fig. 3, but now obtained by diagonalizing

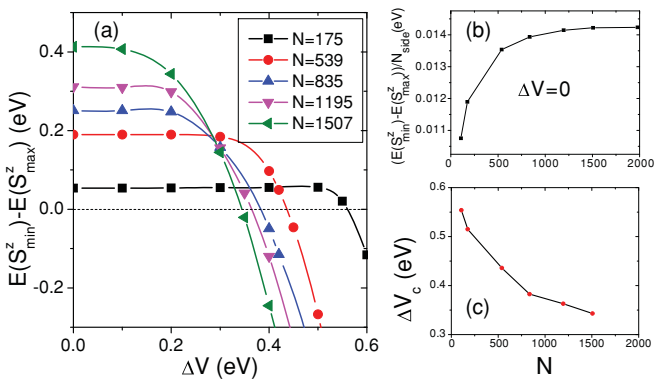

FIG. 4. (Color online) Size dependence of ferromagnetic-antiferromagnetic transition. (a) FM-AFM energy difference as a function of potential difference ΔV, up to $N = 1507$ atoms. (b) For $\Delta V = 0$, the FM-AFM energy gap per number of side atoms N_{side} approaches 14.3 meV. (c) Critical value ΔV_c where the transition occurs as a function of number of atoms N.

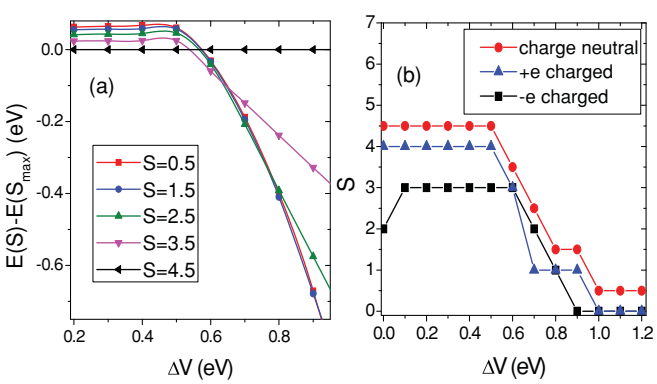

FIG. 5. (Color online) Configuration interaction results. (a) Energies of states for different total spin S as a function of potential difference ΔV between the layers, with respect to the ferromagnetic configuration $S_{\max} = 4.5$ for the same system as in Fig. 3. (b) Ground state total spin S as a function of ΔV for the charge neutral system, $-e$ charged system, and $+e$ charged system.

the many-body Hamiltonian. We observe two main differences from the mean-field Hubbard results: (i) at low ΔV, the antiferromagnetic configuration $S = 1/2$ is no longer the first excited state. Although the AFM-FM energy gap is still comparable to the Hubbard result, other spin excitations are now closer to the ground state due to correlation effects. (ii) The ground state spin transitions do not occur as abruptly as in a Hubbard model. As shown in Fig. 5(b), the total spin of the charge neutral system (red color online, solid line with circles) evolves toward the minimum spin state $S = 1/2$ gradually between $\Delta V = 0.5$ and 1.0 eV. This is mainly due to long-range interactions. As the electrons are transferred one by one from the top layer into the bottom layer, they leave a positively charged hole behind which makes it harder to transfer more electrons. We note that this behavior of gradual spin transition is also obtained within a mean-field Hubbard model with long-range interactions included (not shown). Finally, in Fig. 5(b), we also study the effect of charging the BTGQD system. The asymmetry between magnetic moment of $+e$ and $-e$ charged systems reflects the correlation induced spin depolarization process that occurs in single layer TGQDs as discussed in our previous works.[15]

V. SUMMARY

In summary, we demonstrate that the graphene bilayer triangular quantum dots exhibit a shell of degenerate states at the Fermi level. At half filling, the shell is maximally spin polarized. By the application of a vertical electric field, the total spin of the bilayer structure can be turned off or reduced to a single localized spin, a qubit isolated from contacts and free from interaction with nuclear spins. This opens new possibilities in the area of spintronics and quantum information processing.

ACKNOWLEDGMENT

The authors thank NRC-CNRS CRP, Canadian Institute for Advanced Research, Institute for Microstructural Sciences, and QuantumWorks for support. P.P. acknowledges financial support from fellowship cofinanced by European Union within European Social Fund. This work was financed from the sources granted by the Department of Scientific Research for science development in the years 2010–2012, as a research project, Grant No. NN202 48839.

*devrim.guclu@nrc.ca or pawel.hawrylak@nrc-cnrc.gc.ca

[1] P. R. Wallace, Phys. Rev. **71**, 622 (1947).
[2] K. S. Novoselov, A. K. Geim, S. V. Morozov, D. Jiang, Y. Zhang, S. V. Dubonos, I. V. Grigorieva, and A. A. Firsov, Science **306**, 666 (2004).
[3] K. S. Novoselov, A. K. Geim, S. V. Morozov, D. Jiang, M. I. Katsnelson, I. V. Grigorieva, S. V. Dubonos, and A. A. Firsov, Nature **438**, 197 (2005).
[4] Y. B. Zhang, Y. W. Tan, H. L. Stormer, and P. Kim, Nature **438**, 201 (2005).
[5] S. Y. Zhou, G. H. Gweon, J. Graf, A. V. Fedorov, C. D. Spataru, R. D. Diehl, Y. Kopelevich, D. H. Lee, S. G. Louie, and A. Lanzara, Nat. Phys. **2**, 595 (2006).
[6] A. H. C. Neto, F. Guinea, N. M. R. Peres, K. S. Novoselov, and A. K. Geim, Rev. Mod. Phys. **81**, 109 (2009).
[7] D. M. Hoffman, P. C. Eklund, R. E. Heinz, P. Hawrylak, and K. R. Subbaswamy, Phys. Rev. B **31**, 3973 (1985).
[8] P. Hawrylak, Solid State Commun. **63**, 241 (1987).
[9] L. A. Ponomarenko, F. Schedin, M. I. Katsnelson, R. Yang, E. W. Hill, K. S. Novoselov, and A. K. Geim, Science **320**, 356 (2008).
[10] J. Lu, P. S. E. Yeo, C. K Gan, P. Wu, and K. P. Loh, Nat. Nanotechnol. **6**, 247 (2011).
[11] J. Guttinger, T. Frey, C. Stampfer, T. Ihn, and K. Ensslin, Phys. Rev. Lett. **105**, 116801 (2010).
[12] B. Wunsch, T. Stauber, and F. Guinea, Phys. Rev. B **77**, 035316 (2008).
[13] J. Akola, H. P. Heiskanen, and M. Manninen, Phys. Rev. B **77**, 193410 (2008).
[14] M. Ezawa, Phys. Rev. B **81**, 201402 (2010).
[15] A. D. Güçlü, P. Potasz, O. Voznyy, M. Korkusinski, and P. Hawrylak, Phys. Rev. Lett. **103**, 246805 (2009).
[16] A. D. Güçlü, P. Potasz, and P. Hawrylak, Phys. Rev. B **82**, 155445 (2010).
[17] P. Potasz, A. D. Güçlü, and P. Hawrylak, Phys. Rev. B **81**, 033403 (2010).
[18] O. Voznyy, A. D. Güçlü, P. Potasz, and P. Hawrylak, Phys. Rev. B **83**, 165417 (2011).
[19] J. Fernandez-Rossier and J. J. Palacios, Phys. Rev. Lett. **99**, 177204 (2007).
[20] W. L. Wang, S. Meng, and E. Kaxiras, Nano Lett. **8**, 241 (2008).
[21] D. C. Elias *et al.*, Science **323**, 610 (2009).
[22] E. McCann, D. S. L. Abergel, and V. I. Falko, Solid State Commun. **143**, 110 (2007).
[23] T. Ohta, A. Bostwick, T. Seyller, K. Horn, and E. Rotenberg, Science **313**, 951 (2006).
[24] E. V. Castro, K. S. Novoselov, S. V. Morozov, N. M. R. Peres, J. M. B. Lopes dos Santos, J. Nilsson, F. Guinea, A. K. Geim, and A. H. Castro Neto, Phys. Rev. Lett. **99**, 216802 (2007).
[25] J. B. Oostinga, H. B. Heersche, X. Liu, A. F. Morpurgo, and L. M. K. Vandersypen, Nat. Mater. **7**, 151 (2007).
[26] K. F. Mak, C. H. Lui, J. Shan, and T. F. Heinz, Phys. Rev. Lett. **102**, 256405 (2009).
[27] Y. Zhang, T. T. Tang, C. Girit, Z. Hao, M. A. Martin, A. Zettl, M. F. Crommie, Y. R. Shen, and F. Wang, Nature **459**, 820 (2009).
[28] R. T. Weitz, M. T. Allen, B. E. Feldman, J. Martin, and A. Yacoby, Science **330**, 812 (2010).
[29] E. V. Castro, K. S. Novoselov, S. V. Morozov, N. M. R. Peres, J. M. B. Lopes dos Santos, J. Nilsson, F. Guinea, A. K. Geim, and A. H. Castro Neto, J. Phys. Condens. Matter **22**, 175503 (2010).
[30] L. M. Zhang, Z. Q. Li, D. N. Basov, M. M. Fogler, Z. Hao, and M. C. Martin, Phys. Rev. B **78**, 235408 (2008).
[31] J. M. Pereira, P. Vasilopoulos, and F. M. Peeters, Nano Lett. **7**, 946 (2007).
[32] E. V. Castro, N. M. R. Peres, J. M. B. Lopes dos Santos, A. H. Castro Neto, and F. Guinea, Phys. Rev. Lett. **100**, 026802 (2008).

[33]B. Sahu, H. Min, A. H. MacDonald, and S. K. Banerjee, Phys. Rev. B **78**, 045404 (2008).
[34]A. R. Wright, J. C. Cao, and C. Zhang, Phys. Rev. Lett. **103**, 207401 (2009).
[35]H. Chiba, D. Chiba, F. Matsukura, T. Omiya, E. Abe, T. Dietl, Y. Ohno, and K. Ohtani, Nature **408**, 944 (2000).
[36]A. Rycerz, J. Tworzydo, and C. W. J. Beenakker, Nat. Phys. **3**, 172 (2007).
[37]Y. W. Son, M. L. Cohen, and S. G. Louie, Nature **444**, 347 (2006).
[38]B. Trauzettel, D. V. Bulaev, D. Loss, and G. Burkard, Nat. Phys. **3**, 192 (2007).
[39]H. Sahin, R. T. Senger, and S. Ciraci, J. Appl. Phys. **108**, 074301 (2010).
[40]L. A. Agapito1, N. Kioussis, and E. Kaxiras, Phys. Rev. B **82**, 201411(R) (2010).
[41]E. H. Lieb, Phys. Rev. Lett. **62**, 1201 (1989).